SSRG International Journal of Recent Engineering Science
ISSN: 2349–7157 / https://doi.org/10.14445/23497157/IJRES-V11I4P118

Volume 11 Issue 4, 145-154, Jul-Aug 2024

Original Article

Investigation of a Hybrid-Electric Scooter and Computational Fluid Dynamics Analysis of its Battery Pack Cooling System

Bheru Lal Salvi[1], Jay Upadhyay[2]

[1,2]*Sustainable Energy Research Laboratory (SERL), Department of Mechanical Engineering, College of Technology and Engineering, Maharana Pratap University of Agriculture and Technology, Udaipur, Rajasthan, India*.

[1]*Corresponding author : salvibl@gmail.com*

Received: 19 June 2024 Revised: 03 August 2024 Accepted: 19 August 2024 Published: 31 August 2024

Abstract - *The need for a clean environment leads to the incorporation of electric vehicles in the public fleet. In the present study, a conventional gasoline fuelled scooter was converted into a Hybrid-Electric Scooter (HES), and its performance study was carried out. Furthermore, a Computational Fluid Dynamics (CFD) study was carried out for heat generation and cooling of the battery pack and its cells within it. The scooter can be operated in single mode on electric power or engine power as well as parallel mode on electric motor and engine power. During vehicle driving, it was observed that battery temperature increased with an increase in speed and time of travel. The battery cell surface temperature reached above 55°C. A Computational Fluid Dynamics (CFD) simulation study for cooling both the battery pack surface and cell surface inside the battery pack at different air velocities of 15 km/h and 25 km/h has shown promising results in reducing the temperature of cell surface and pack surface about 3-4°C as compared to the isolated or battery with restricted airflow. For this air conduit design, modification is required depending on the space and requirement. The converted hybrid-electric scooter (HES) can use the existing vehicle infrastructure and fairly reduce the dependence on fossil fuels. In rural areas, the HES may be charged during the day with a solar PV system installed on the farmer's land. The HES can also be operated with conventional fuel when the battery is discharged.*

Keywords - *E-scooter, Hybrid-electric scooter, Battery cooling, CFD analysis of battery, Battery pack.*

1. Introduction

Air pollution caused by road traffic is a major public health concern, with motor vehicle exhaust emissions being the main source of pollutants such as carbon monoxide, nitrogen oxide, and sulphur oxides [1, 2]. These harmful gases have a negative impact on people's health over time and contribute to illness and death in society. Motorist vehicles are the main source of carbon monoxide. The transportation system faces various issues in India. One of the significant issues is the adverse impact of transportation on the environment and climate change. Private vehicles, including scooters, contribute to more than half of the air pollution, resulting in rising mean temperatures, major weather events, and many other effects. Additionally, the rising cost of energy and traffic congestion are also common problems in most urban areas of India. Electric vehicles have been in existence since the 19th century, with Robert Anderson's motorized carriage built between 1832 and 1839 in Scotland. However, due to high costs, low speed, and short range, their demand declined worldwide. Today, automobile companies face a significant challenge of environmental sustainability, and regulations have been implemented to encourage the use of electric vehicles to reduce greenhouse gas emissions and fossil fuel dependence. By adopting a revolutionary shared-connected electric mobility solution, the Indian automobile industry aims to achieve a 100 percent pure electric vehicle by the time India celebrates its 100th year of independence. However, battery degradation and charging infrastructure remain major obstacles that must be addressed. The thermal management study of densely-packed EV batteries with forced air-cooling strategies was carried out by Lu et al. [3], who reported that battery cooling is required for better performance and safe operation. Research is going on to determine whether the network infrastructure is sufficient in the new condition and charging infrastructure [4]. The battery operates between max. 53 V to min. 43V, as reported by Affanni et al. [5].

2. Hybrid electric scooter

Hybrid electric scooters are vehicles that integrate with an internal combustion engine and an electric motor, allowing for more efficient use of energy. The battery can be charged by the engine or regenerative braking [6]. Various designs and simulation models have been developed to improve fuel

consumption rates and understand the effectiveness of series-parallel connections [7]. HES offers quick and smooth acceleration and emits less CO_2, making them environmentally friendly. Research studies have been conducted to improve the design of ES motors and test the performance of lightweight electric vehicles. Additionally, studies have shown that ES can be used for commuting and recreational travel. Furthermore, voltage and current control systems have been developed to improve the performance of ES batteries.

Table 1. Comparison of electric and petrol fuel scooters

Comparison Point	Electric powered scooter	Petrol fuel scooter
CO_2 Release	Nearly zero	Comparatively high
Fuel charges	Low priced	High priced
Maintenance	Cheap	Costly
No of moving parts	Few	Many
Friction losses	Low	High
Performance	Better	Good
Range	More range in the city	More range on highways
Purchase cost	Expensive	Cheaper than EV's

Electric power for vehicular applications introduces a cleaner energy system in the transportation fleet. The present work includes the selection of a battery and conversion of a gasoline fuelled scooter into a Hybrid Electric Scooter (HES). Additionally, the performance and battery cooling studies were carried out using Ansys Fluent.

3. Materials and methodology

A gasoline fuelled scooter was converted into a hybrid-electric scooter. Then, its performance study and computational fluid dynamics study were carried out to find out the heating and cooling requirements within the battery pack. A gasoline fuelled scooter, TVS Scooty Teenz, made in 2010, powered by a 2-stroke, single-cylinder, forced air-cooled SI engine equipped with front and rear drum brakes and 10-inch wheels, was selected for this study. The Scooty Teenz, with an analogue speedometer and odometer, hand-operated throttle and brakes, a two-person capacity, and front suspension, were of the link type. In order to satisfy the power and range requirements, a motor and battery of comparable characteristics were chosen.

3.1. Selection of motor

Electric scooters commonly use either Brushed Direct Current (BDC) motors or Brushless Direct Current (BLDC) motors. BLDC motors, based on newer technology, offer several advantages, including higher efficiency, better power-to-weight ratio, and reduced noise compared to BDC motors. These factors make BLDC motors a preferred choice for electric scooters, providing sufficient power and performance while maintaining a comfortable and efficient riding experience [8]. The required power of the motor is given by Equation (1).

$$P = \tau * \omega \quad (1)$$

Where P = power (W), τ = torque (Nm) and ω = angular momentum (rad/s). The angular momentum is given by Equation (2).

$$\omega = \frac{v}{r} \quad (2)$$

Force is calculated using the coefficient of static friction value as 0.7 and the normal reaction on the wheel in Equation (3).

$$F = \mu * N \quad (3)$$

The overcoming torque is given by Equation (4).

$$\tau = F * r \quad (4)$$

From the findings of Equations (3) and (4), the power was calculated by using Equation (1). Where F = force (kg), N= normal force (N), μ= coefficient of friction, V = velocity (km/h), r = radius of wheel (m), τ = torque (Nm), ω = angular momentum (rad/s), and P = power (W). Three constraints were set by varying the force applied on the wheel to calculate the power required for the motor. The motor selected for the Hybrid-Electric Scooter (HES) was a 750W in-wheel hub BLDC motor having a size which can fit the 254 mm wheel diameter.

3.2. Selection of battery pack

For selecting the battery for a Hybrid Electric Scooter (HES), the key factors considered were high power-to-weight ratio, power efficiency, wide availability, recyclability, safety, performance in extreme temperatures, lifespan, and cost. Li-ion batteries were compared based on specific energy, specific power, safety, performance, lifespan, and cost, with specific energy being a crucial factor affecting driving range [9, 10]. Battery pack capacity is determined by the total electricity generated through battery reactions, showcasing the battery's power output under specific discharge conditions. The selection of the battery pack considers motor requirements, range, and lifespan. The capacity of the battery pack is calculated by using Equation (5).

$$P_b = P_m * t_T \quad (5)$$

Where P_m = motor power (W), P_b = battery power (Wh) and t_T = travel time. Now, the current drawn by the motor is given by Equation (6).

$$I_m = \frac{P_m}{V} \quad (6)$$

Where P_m = motor power (W), V = motor voltage (v), and I_m = motor current (A).

Further, considering the current losses during acceleration as 5-10%, the maximum current drawn by the

motor is given by Eq. (7).

$$I_{max} = \frac{I_m}{0.90} \quad (7)$$

Finding the power required by the motor to run at the desired top speed is given by Eq. (8).

$$P_m = V * I_{max} \quad (8)$$

Now, designing the battery pack for a certain kilometre range, the travel time is given by Equation (9).

$$t_T = \frac{\text{desired travel } range\ (km)}{average\ speed\ (kmph)} \quad (9)$$

Also, considering that the charging and discharging efficiency is about 85% from Equations (5) and (9), the battery pack capacity is given by Equation (10).

$$Battery\ pack\ capacity = \frac{P_b}{0.85} \quad (10)$$

As shown by Equation (5), the battery pack capacity is directly related to the power of the motor and the speed at which the motor is supposed to be operated. A definite power motor has limited top speed. So, for the selection of battery pack, the vehicle travelling range was assumed to be 80 km. The selected battery pack has the capacity of 20 Ah and 48V, which consists of cells 13 numbers in series and 12 numbers in parallel connection, making it a pack of 156 cells, with a battery pack of dimensions 275x245x100mm.

3.3. Conversion of old scooter to Hybrid Electric Scooter

The selected Petrol fuelled scooter, as described above, was converted into a Hybrid Electric Scooter (HES) for developing the electric vehicle by using the present vehicle infrastructure to reduce the environmental impact caused by conventional internal combustion engines. The schematic diagram of HES is shown in Figure 1.

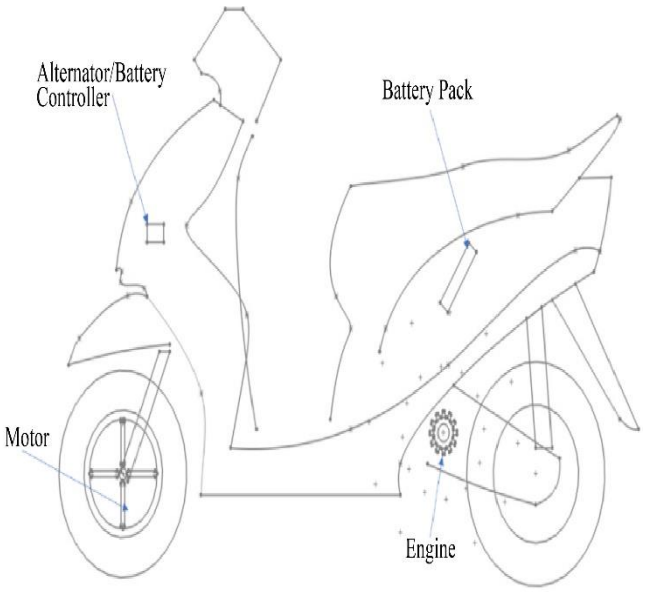

Fig. 1 Schematic diagram of Hybrid Electric Scooter

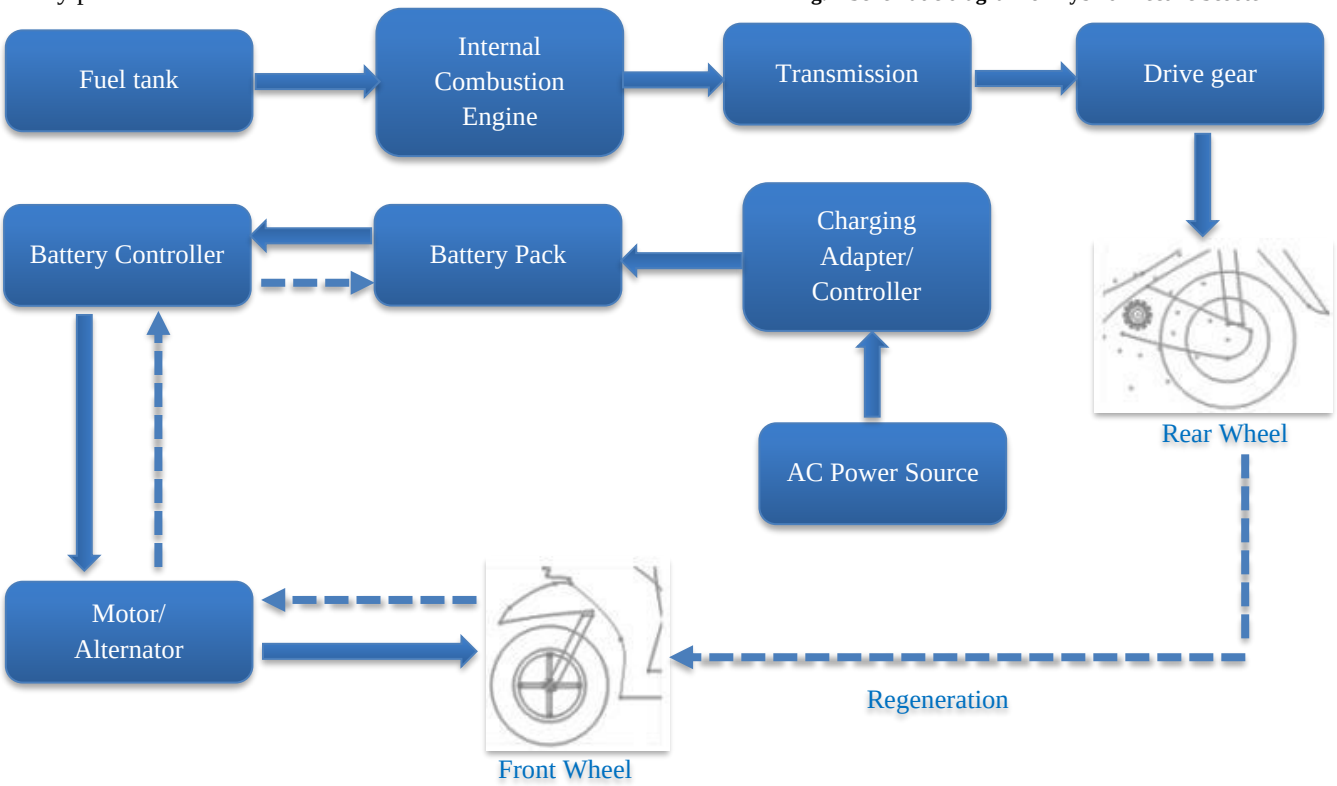

Fig. 2 Power-train configuration of Hybrid Electric Scooter

The BLDC motor was attached to the front wheel, which drives the scooter in EV mode. The motor was placed with a few arrangements, such as changing the wheel within the wheel hub motor and removing the old front link-type suspension to add a new damper suspension. The battery placed in the scooter's boot space was equipped with a Battery Management System (BMS) that automatically cuts off power to the motor if the battery temperature exceeds safe limits, preventing overheating and fire hazards. The controller manages the depth of discharge and BMS operations.

3.4. Power train configuration of Hybrid Electric Scooter

The Hybrid Electric Scooter (HES) uses the battery to power the BLDC motor and the engine as a backup power source for the rear wheel when there is no electricity. The engine also charges the battery through energy regeneration while driving in internal combustion engine mode [6]. The power train configuration of HES is shown in Figure 2.

3.5. Testing the hybrid electric scooter

The converted Hybrid-Electric Scooter (HES) was tested at Maharana Pratap University of Agriculture and Technology, Udaipur. The testing parameters included measurement of temperatures at the battery surface, battery's cell surface and motor surface, and distance travelled at different speeds until the battery was drained up to 43 V, which is the lower limit for battery drain as suggested for the Battery Management System (BMS). For each test, the battery was fully charged, and each test was carried out for 10 minutes. The surface temperature of the battery cells and the pack was measured by using an IR-based temperature gun (Temperature range of -50°C to 750°C, with least count of 0.01°C). An openable window was created in the battery pack to get excess for the battery cell. For tracking and measuring the range and speed of HES the smartphone GPS with the Zeopoxa tracking application was used for accurate travel distance measurement.

3.6. Heat generation in battery

During battery discharge, heat is generated due to enthalpy change and chemical reactions. The flow of current through the resistive component of the cells produces Joule heat, leading to an increase in the temperature of the cell and the battery pack.

Joule heating is considered a parameter for heat generation in battery packs (source: Diyguru) [11].
The joule heating Q in the cell is calculated by using Eq. (11).

$$Q = I_c^2 * \Omega \quad (11)$$

Where Q = Heat generation (W), I_c = Cell current (A) and Ω = end resistance (Ohm). Based on motor power and voltage, the rated current of motor I_r is calculated using Equation (12).

$$I_r = \frac{P}{V} \quad (12)$$

Now, find the charge rate C_{rate} using Equations (13) and (14).

$$C_{rate} = \frac{I_r}{I_b} \quad (13)$$

$$C_{peak} = \frac{I_p}{I_b} \quad (14)$$

Considering each cell capacity, the cell current is given by Eq. (15).

$$I_c = each\ cell\ capacity * C_{rate} \quad (15)$$

After finding the cell current and considering the standard end resistance of a cell, the Joule heating of a cell is calculated by using Eq. (11). Where I_r = Rated motor current (A), I_p = Peak motor current (A), I_b = Battery pack current (A), C_{rate} rated = Charge rate, C_{rate} peak = Charge rate, P = Motor power, and V = Motor voltage.

3.7. Steady State Thermal analysis of battery cell in ANSYS

For heat transfer study on the cell surface, the steady state thermal study was performed on the cell by using Ansys 2021 R1 software. The value of heat transferred was calculated by Joule heating factor in watts by using Equation (11) [12]. A CAD model of the battery pack was imported. The temperature distribution in the cell can be seen in Ansys software using steady-state thermal analysis, using steps shown in Figure 3. A grid-independent study was performed on the CAD model of a cell in Ansys, where no such deviation in results was noticed when meshing with fine and coarse mesh. So, to make the solution, the fast coarse mesh of 0.002m mesh size with 8226 nodes and 4472 elements is used on the cell in Ansys.

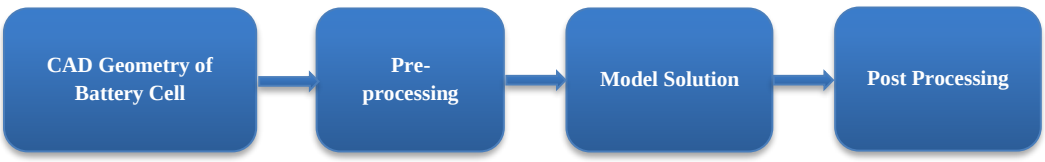

Fig. 3 Steady-state thermal methodology

3.8. Convection heat transfer on cell surface

The convection heat transfer helps to know the temperature with factors considering material heat transfer coefficient, heat and initial temperature (Giedt, 2014) [13]. For finding the temperature of the cell, the convection heat transfer equation was used considering Joule heating results E. The convection heat transfer equation is given in Eq. (16).

$$Q = hA(T_s - T_f) \quad (16)$$

Where, Q = Heat transfer (W), h = Convection heat-transfer coefficient (W/m^{2}K), A = Exposed surface area (m^2), Ts = Surface Temperature (°C), and T_f = Fluid Temperature (°C). Further, the value of Q is found by using Equation (11). Then, the temperature of the battery cell is given by Equation (17).

$$T_s = \left(\frac{Q}{hA}\right) + T_f \quad (17)$$

3.9. CFD analysis of battery cooling in Ansys

The temperature rise in a Li-ion battery can lead to thermal runaway and fire, with a trigger warning temperature of 60°C and a critical limit of 80°C, according to Tete et al. [14]. To obtain more precise results and heat distribution patterns around the cell and battery, the CFG analysis is required.

The CAD models of the battery cell and pack were created in Ansys, and a CFD analysis was carried out using boundary conditions, as shown in Table 2. A grid-independent study was performed where the fine mesh of mesh size of 0.001m with 117636 nodes and 113344 elements on the cells inside the pack showed better results and was selected. However, in the case of the battery pack, there is no such variation in results, so the coarse mesh of 0.003 m size with 2392 nodes and 7477 elements was selected for faster processing; the meshing of the models is shown in Figures 4(a), (b) and (c).

The system included 25 surfaces with 3 mm spacing and considered various inlet airflow speeds. CFD method was used to calculate the flow field and temperature field, considering the turbulence flow due to a Reynolds number above 3000 [15]. Boundary conditions included constant temperature airflow inlet, pressure outlet, non-slip conditions, and adiabatic conditions on the surrounding walls. The air inlet and battery pack walls are shown in Figure 5 (a) and (b). The location for battery cell surface temperature measurement is shown in Figure 5(c).

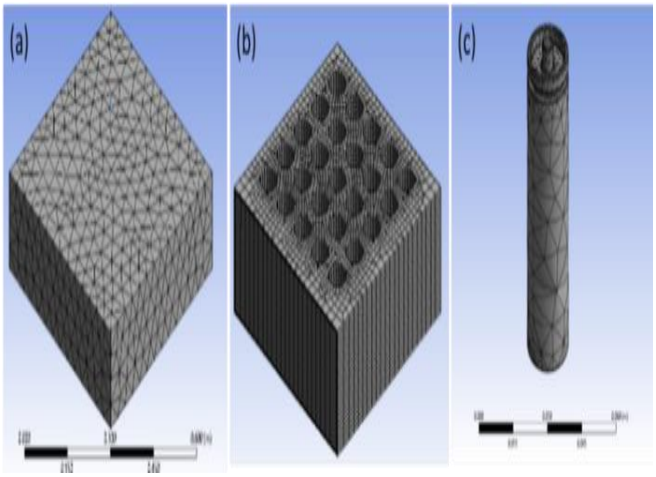

Fig. 4 Meshed model of (a) battery pack and (b) cells inside pack

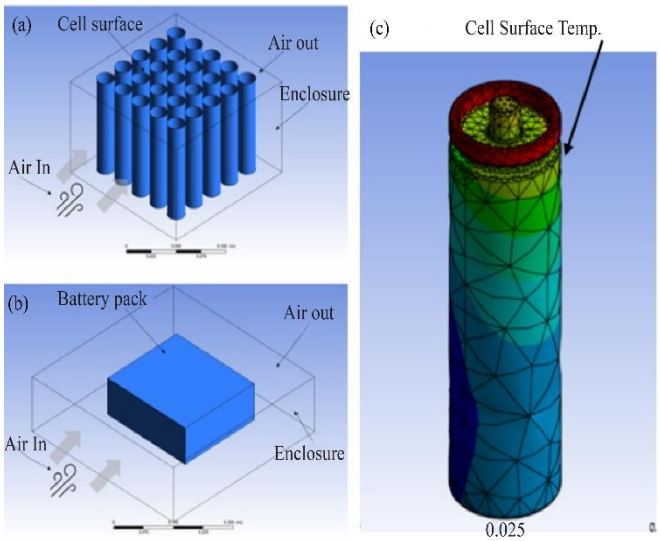

Fig. 5 Airflow direction for (a) cells inside the battery pack, (b) wall of the battery pack and (c) location of battery cell temperature measurement

3.10. Experimental validation of the CFD model:

The experimental temperature was measured by an IR temperature gun, as explained in Section 3.5, and the CFD results were identified at a similar location in the CFD model, as shown in Figure 5(c). The experimental results and CFD results for battery pack temperature (battery surface temperature and cell surface temperature) were compared to validate the CFD model. It can be observed from Figure 6 that the temperature difference between the experimental and CFD results is within the 5% error limit, which is acceptable. Hence, the CFD model was validated, and further analysis was carried out by changing boundary conditions, as shown in Table 2. The battery's heat source was replaced with a temperature surface, and iterations were performed for further simulation study.

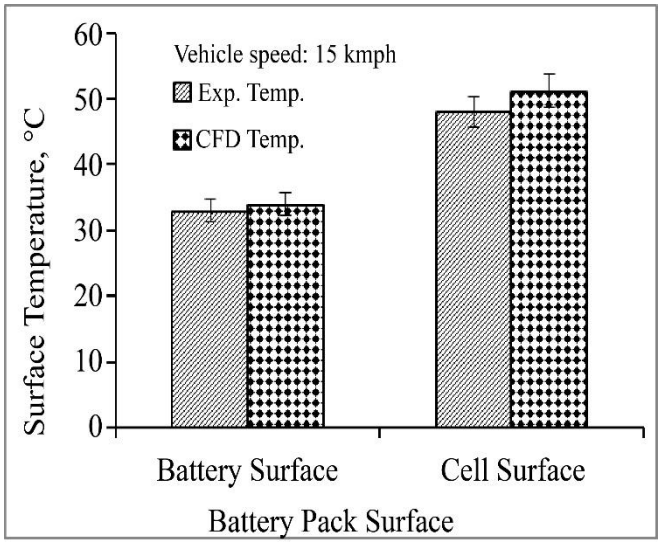

Fig. 6 Experimental and CFD-based surface temperature results for model validation

Further, CFD simulation was performed to study the effects of air velocity on air cooling of battery with certain temperatures and air velocity with the boundary condition, as shown in Table 2. The air inlet velocity was calculated based on the vehicle speed and, accordingly, joule heating for different amounts of current drawn.

Table 2. Boundary conditions

No. of cases	Case-1 (Vehicle Stationary)	Case-2 (Vehicle moving)	Case-2 (Vehicle moving)
Speed of vehicle (km/h)	0	15	25
Airspeed (m/s)	0	4.16	6.94
Joule heating (w)	0	0.08	0.19
Initial temp. (°C) of battery surface	29.5	32.6	33.7
Numerical temp. (°C)	29.5	35	45

4. Results and discussion

The experimental and analytical results on the impact of varying speeds of the Hybrid Electric Scooter (HES) on the temperature of the battery and motor were presented. It also discusses the effects of increased battery temperature and explores cooling methods both inside and outside the battery case. Different results are presented with a 5% error of measurement.

4.1. Motor power

The numerical calculations for motor power consider different payload conditions: 120 kg, 150 kg, and 170 kg (load including scooter's mass and two persons), as shown in Figure 7. The calculated results suggest that for a certain weight on wheels, the power of the motor linearly increases to match the speed of vehicles; the summarized results show that a high-power motor is required to carry heavy weight at high speed.

4.2. Battery pack capacity

The calculation of battery pack capacity was carried out for a Hybrid-Electric Scooter (HES) for a fixed range of 80 km considering different power of the motor, continuously working on their top speed. To identify the battery pack capacity for a range of 80 km considering the top speed and motor power, a graph plotted between battery pack capacity and the speed of the vehicle is shown in Figure 8. The calculated results show that the capacity of the battery pack depends on the power of the motor.

There is an increased requirement for battery pack capacity with respect to the increase in the driving speed of vehicles. The calculated capacity of the battery pack for an 80 km driving range with 50 kmph of driving speed is about 2.65 kWh.

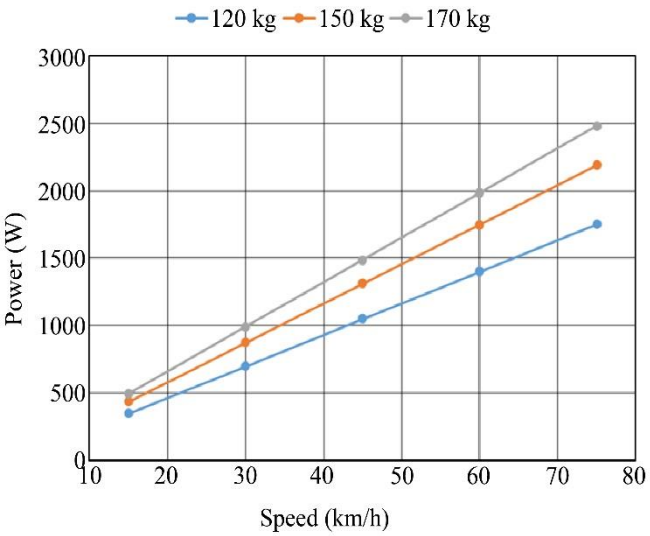

Fig. 7 Required motor power w.r.t. desired vehicle speed

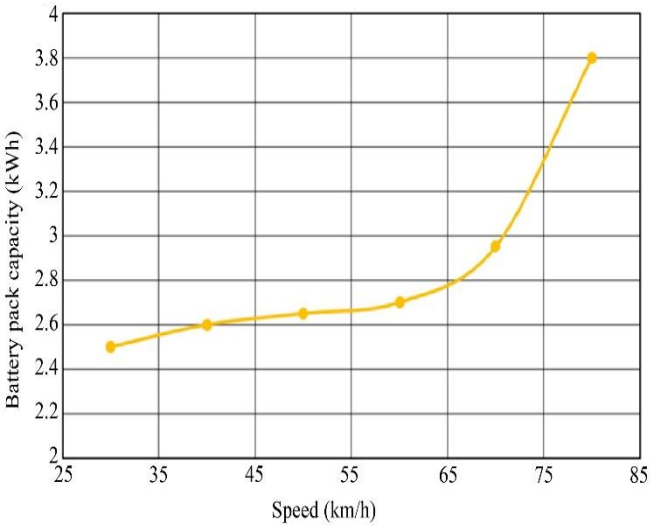

Fig. 8 Battery pack capacity w.r.t. vehicle speed for 80 km range

4.3. Performance of Hybrid Electric Scooter

4.3.1. Temperature variation in battery pack and motor during vehicle operation

Testing of HES was done to carry out the study of the driving characteristics of vehicles to know the discharge rate, speed, range, and temperature of different areas. Vehicle road testing was carried out at various speeds. The temperature of the battery surface, motor surface and vehicle body were observed at different driving speeds, as shown in Figure 9. It can be observed from the test results that as the average speed of the vehicle increases, the battery surface temperature and motor surface temperature increase comparatively slowly, but the battery cell temperature increases rapidly. The battery surface temperature and motor surface temperature remain relatively stable due to the cooling effect of forced convection. On the contrary, the cells are arranged in the battery pack, and these are not exposed to forced air due to the protection of cells from moisture and dust. Due to that, the better cell temperature is

increasing w.r.t. vehicle speed. Even at higher speeds, the driving may cause very high battery cell surface temperature beyond the critical temperature of 80 °C [14], which may cause the cells to fire. Therefore, a proper cooling arrangement for battery cells is required.

4.4. Performance of battery during charging and discharging

The vehicle's battery is drained while the vehicle is running, considering various factors such as speed and inclined roads. The battery's controller maintains a voltage cut-off at around 43V to prevent the over-discharging. The battery discharging below 43V requires a higher power charger to charge the battery again. The variation in battery voltage and battery surface temperature during battery charging is shown in Figure 10. It can be observed that approximately 150 minutes are required to charge the battery from 44.5V to 53V using a 220V charger. While charging the battery continuously, the battery surface temperature increases with charging time. The battery surface temperature rose from 29.5°C to 48 °C with an increase in voltage from 43V to 53V in 150 min. The electric vehicle's batteries are charged during nighttime when the vehicle is not running. During this, forced airflow on the battery is absent, which may lead to battery cooling problems. Overcharging sometimes causes a rise in temperature and the battery to go on fire.

4.5. Internal heat generation and temperature rise during battery discharging

During vehicle operation, battery discharges and Joule heating take place. The major factors considered are power, current, and battery crate. The Joule heating varies with respect to current drawn from 14Ah to 46Ah, leading to heat generation from 0.1W at the initial stage to 0.85W when the current drawn from the motor is at its peak, as shown in Figure 11.

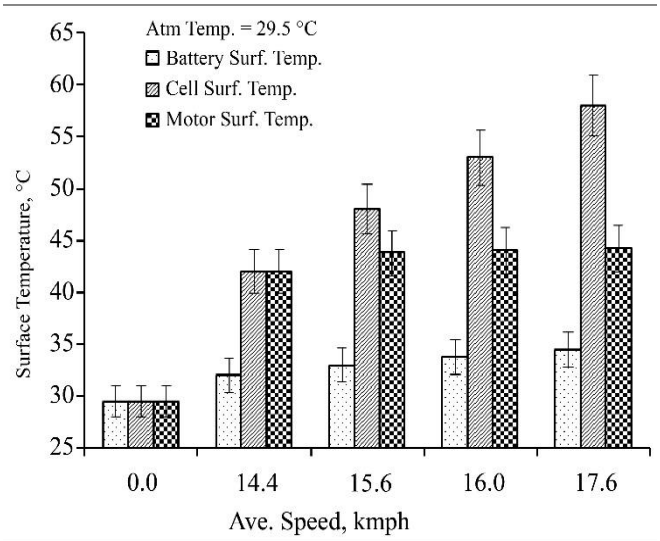

Fig. 9 Test characteristics of the vehicle in which average speed is compared against the temperature of battery, motor and vehicle body

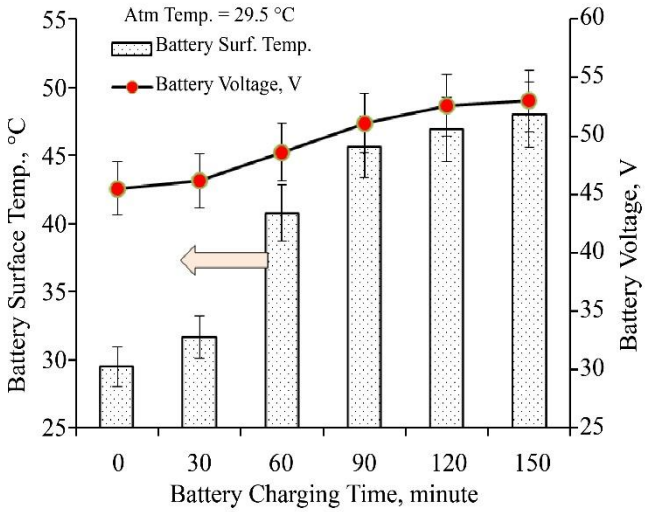

Fig. 10 Variation in battery voltage and battery surface temperature w.r.t. charging time during battery charging

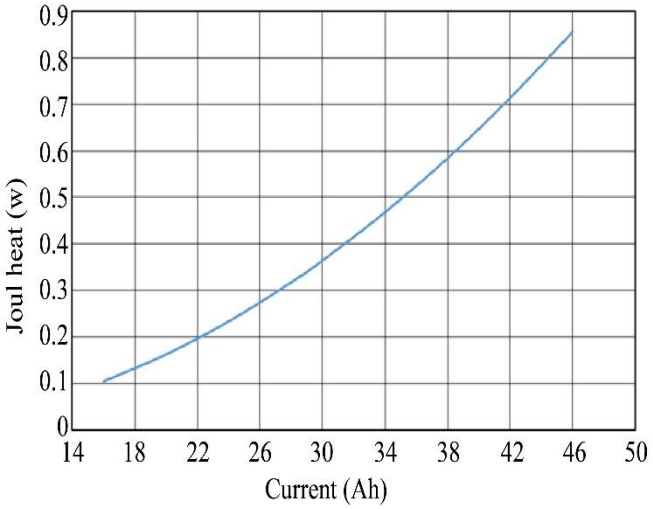

Fig. 11 Heat generation in battery w.r.t. current drawn from battery by motor

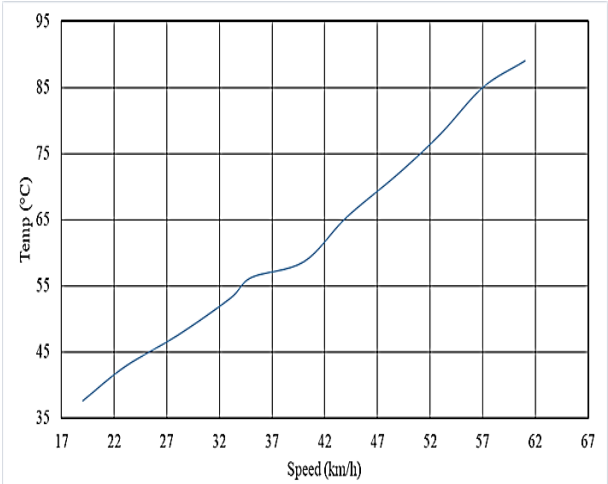

Fig. 12 Increase in temperature in battery w.r.t. speed of vehicle

The battery temperature versus the speed of the vehicle is shown in Figure 12. The results obtained show that an increase in temperature in the battery is due to increasing the speed of the scooter, running the scooter at 55kmph, and raising the temperature above 70°C. Even if this exceeds the critical temperature limit, i.e., 80°C of battery, when operated at higher speeds, then a thermal runaway may occur, as reported by Tete et al. [14]. This shows the adverse effect of high temperatures in the battery, or even at low temperatures, the efficiency of the battery is affected. Therefore, proper cooling of the battery is necessary.

4.6. CFD simulation

The CFD simulations were performed to find out the optimum airflow and understand the heat distribution pattern in the battery cell. To know the temperature distribution on the cell surface, steady-state thermal analysis was done, and the temperature distribution on the surface is shown in Figure 13, which indicates the heat generated inside the cell was transferred to the cell surface, which means cooling the cell surface directly cools the cell heat inside. ANSYS Fluent solution was used to simulate solutions for all the boundary conditions. In the present work, the solution method was kept simple. Hybrid initialization was done, and calculations were done for 50 iterations, where the solution was discussed. Then, the results were processed and observed using the post-processor in ANSYS fluent, and the results simulated were computed, i.e., temperature volume rendering, velocity streamline, and contours. The streamlines for velocity comparison for airflow distribution for both cells and battery pack enclosures are shown below in Figure 14.

From the simulation study done so far and comparing the airflow, it can be said that the developed cooling system performs well and is verified for the decrease in the temperature of the battery. The comparison shows the increase in cooling with the increase in airflow and the increase in air distribution inside the enclosure. These results helped to make the air-cooling system more feasible.

The effects of air cooling on cells and battery pack surface with airflow when the vehicle is stationary and when the vehicle is moving are presented. The temperature distribution in the cells of the battery is shown in Figure 15, and the temperature distribution on the battery surface is shown in Figure 16. It is observed from the figures that battery surface and cell temperature decreased with respect to an increase in air inlet velocity, which is a function of vehicle speed. This result helps to compare the case of cooling when the battery cells are isolated and when they are open for airflow; the decrease in temperature lowers the chances of thermal runaway and fire in the battery. It can be seen that the decrease in temperatures of the battery cells and battery pack directly depends on the airflow velocity. These results will help in better designing of air conduits and cooling arrangements. As a result, the efficiency and life of the battery would increase.

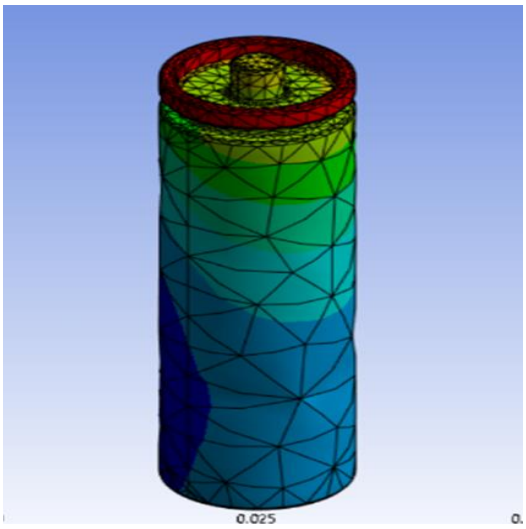

Fig. 13 The heat distribution on the cell surface

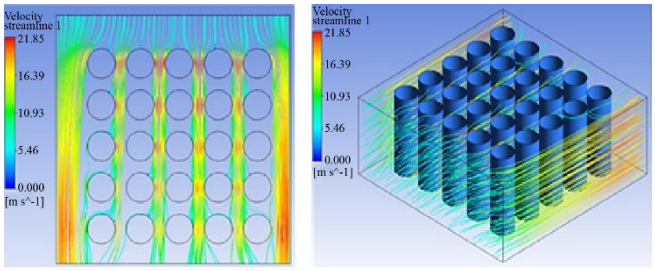

(a) Velocity distribution streamlines inside cell enclosure

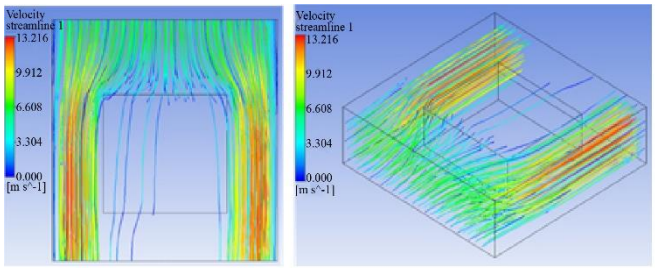

(b) Velocity distribution streamlines inside battery pack enclosure

Fig. 14 Velocity streamlines around battery pack and battery cells

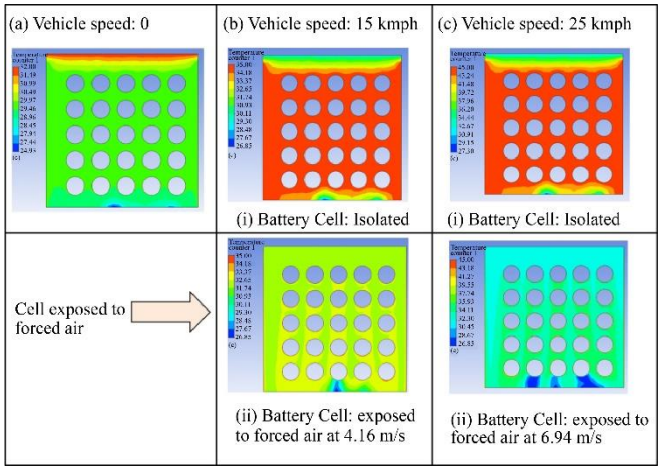

Fig. 15 Effects of forced air cooling on battery cell temperature

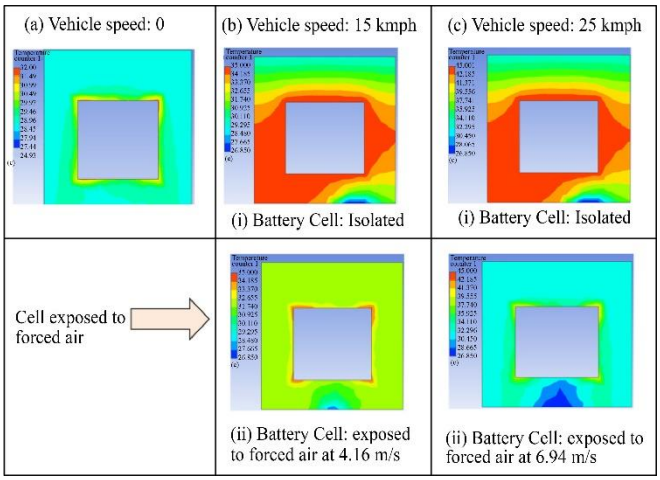

Fig. 16 Effect of forced air cooling on battery pack surface temperature

5. Conclusion

A conventional scooter with a two-stroke engine was successfully converted into a Hybrid-Electric Scooter (HES). When the scooter was being used in the internal combustion engine mode, it charged the battery through power regeneration at the front wheel. The key findings and results are as follows:

- The developed HES possesses the ability to operate in three operating modes: fully electric mode, internal combustion engine mode, and hybrid mode.
- The test results have shown that HES, with a 20Ah battery and 750W BLDC motor, can operate in the range of 30-35 km on a single charge, which makes it sufficient for driving in rural areas and cities.
- For a higher driving range, increased motor power and battery pack capacity are required.
- During vehicle driving, an increase in battery temperature was observed due to an increase in speed and time spent travelling. The battery cell surface temperature reached above 55°C. The increase in temperature above 70°C may cause thermal runaway, which may cause a fire in the battery.
- A CFD simulation study for cooling both the battery pack surface and cell surface inside the battery pack at different air velocities of 15 km/h & 25 km/h has shown promising results of reducing the temperature of the cell surface and pack surface by about 3-4°C. For better cooling, a greater increase in the flow of air is required with proper air conduit design modification.
- Battery packing is required for cells, but proper cooling is also necessary to make a battery pack more efficient and increase life.

The converted Hybrid-Electric Scooter (HES) can use the existing vehicle infrastructure and fairly reduces the dependence on fossil fuels. In rural areas, the HES may be charged during the day with a solar PV system installed on farmers' land. The HES can also be operated with conventional fuel when the battery is discharged.

Funding Statement

The authors gratefully state the financial support received from the New Generation Innovation and Entrepreneurship Development Centre (NewGen IEDC), CTAE, Udaipur, a program of the Department of Science and Technology, Government of India, during the financial year 2021-2022.

References

[1] Fuad Un-Noor et al., "A Comprehensive Study of Key Electric Vehicle (Ev) Components, Technologies, Challenges, Impacts, and Future Direction of Development," *Energies*, vol. 10, no. 8, 2017. [CrossRef] [Google Scholar] [Publisher Link]

[2] Anil Khurana, V. V. Ravi Kumar, and Manish Sidhpuria, "A Study on the Adoption of Electric Vehicles in India: The Mediating Role of Attitude," *Vision*, vol. 24, no. 1, pp. 23-34, 2020. [CrossRef] [Google Scholar] [Publisher Link]

[3] Z. Lu et al., "Thermal Management Of Densely-Packed Ev Battery With Forced Air Cooling Strategies," *Energy Procedia*, vol. 88, pp. 682-688, 2016. [CrossRef] [Google Scholar] [Publisher Link]

[4] Nurullah Aslan, Erdal Kılıc, and Mustafa Şekkeli, "Modeling of Electric Vehicles as A Load of the Distribution Grid," *International Journal of Automotive Science and Technology*, vol. 7, no. 1, pp. 54-62, 2023. [CrossRef] [Google Scholar] [Publisher Link]

[5] Antonio Affanni et al., "Battery Choice And Management For New-Generation Electric Vehicles," *IEEE Transactions on Industrial Electronics*, vol. 52, no. 5, pp. 1343-1349, 2005. [CrossRef] [Google Scholar] [Publisher Link]

[6] Yaohua Li, Ying Wang, and Xuan Zhao, "Modelling And Simulation Study On A Series-Parallel Hybrid Electric Vehicle," *World Electric Vehicle Journal*, vol. 7, no. 1, pp. 133-141, 2015. [CrossRef] [Google Scholar] [Publisher Link]

[7] C. Y. Tseng, C.H. Yu, and Y.T. Lin, "Development of An Auxiliary Mode Powertrain for Hybrid Electric Scooter," *International Journal of Automotive Technology*, vol. 15, no. 5, pp. 805-814, 2014. [CrossRef] [Google Scholar] [Publisher Link]

[8] Lee Ji-Young et al., "In-Wheel Motor Design For An Electric Scooter," *Journal of Electrical Engineering and Technology*, vol. 12, no. 6, pp. 2307-2316, 2017. [CrossRef] [Google Scholar] [Publisher Link]

[9] Yu Miao et al., "Current Li-Ion Battery Technologies In Electric Vehicles And Opportunities For Advancements," *Energies*, vol. 12, no. 6, 2019. [CrossRef] [Google Scholar] [Publisher Link]

[10] Wheelsatev.com, "Battery Pack Capacity Calculation for EVs as per Our Required Range," 2020. [Online]. Available: https://www.wheelsatev.com/2020/09/battery-pack-capacity-calculation-for.html.

[11] Diyguru.org, Electric Vehicle Battery Pack Design and Modelling Course, 2022. [Online]. Available: https://diyguru.org/course/battery-pack-modelling/

[12] P. Cicconi, M. Germani, and D. Landi, "Modeling and Thermal Simulation of a PHEV Battery Module with Cylindrical LFP Cells," *World Electric Vehicle Journal*, vol. 6, no. 1, pp. 175-185, 2013. [CrossRef] [Google Scholar] [Publisher Link]

[13] Warren H. Giedt, "Heat Convection," *AccessScience from McGraw-Hill Education*, 2014. [CrossRef] [Publisher Link]

[14] Pranjali R. Tete, Mahendra M. Gupta, and Sandeep S. Joshi, "Developments in Battery Thermal Management Systems for Electric Vehicles: A Technical Review," *Journal of Energy Storage*, vol. 35, 2021. [CrossRef] [Google Scholar] [Publisher Link]

[15] R.D. Jilte, and Ravinder Kumar, "Numerical Investigation On Cooling Performance Of Li-Ion Battery Thermal Management System At High Galvanostatic Discharge," *Engineering Science and Technology, an International Journal*, vol. 21, no. 5, pp. 957-969, 2018. [CrossRef] [Google Scholar] [Publisher Link]